

Inhibition of tumor metastasis by targeted daunorubicin and dioscin codelivery liposomes modified with PFV for the treatment of non-small-cell lung cancer

This article was published in the following Dove Press journal:
International Journal of Nanomedicine

Yuanyuan Wang¹
Min Fu²
Jingjing Liu²
Yining Yang¹
Yibin Yu¹
Jinyu Li¹
Weisan Pan¹
Lei Fan³
Guiru Li⁴
Xuetao Li²
Xiaobo Wang^{1,3}

¹Department of Pharmaceutics, Shenyang Pharmaceutical University, Shenyang, Liaoning, People's Republic of China;

²School of Pharmacy, Liaoning University of Traditional Chinese Medicine, Dalian, Liaoning, People's Republic of China;

³Department of Pharmacy, 210th Hospital of People's Liberation Army, Dalian, Liaoning, People's Republic of China; ⁴Department of Pharmacy, The Second Affiliated Hospital of Dalian Medical University, Dalian, Liaoning, People's Republic of China

Correspondence: Xiaobo Wang
Department of Pharmaceutics, Shenyang Pharmaceutical University, 103 Wenhua Road, Shenyang 110016, Liaoning, People's Republic of China
Tel/Fax +86 24 2398 6313
Email wxbbenson0653@sina.com

Xuetao Li
School of Pharmacy, Liaoning University of Traditional Chinese Medicine, Shengming I Road 77, Double D port, Dalian 116600, Liaoning, People's Republic of China
Tel +86 411 8589 0170
Fax +86 411 8589 0128
Email lixuetao1979@163.com

Background: Chemotherapy for non-small-cell lung cancer (NSCLC) still leads to unsatisfactory clinical prognosis because of poor active targeting and tumor metastasis.

Purpose: The objective of this study was to construct a kind of PFV peptide modified targeted daunorubicin and dioscin codelivery liposomes, which could enhance tumor targeting and inhibit tumor cell metastasis.

Methods and results: Targeted daunorubicin and dioscin codelivery liposomes were prepared by film dispersion and the ammonium sulfate gradient method. With the ideal physicochemical properties, targeted daunorubicin and dioscin codelivery liposomes exhibited enhanced cellular uptake and showed strong cytotoxicity to tumor cells. The encapsulation of dioscin increased the inhibitory effects of daunorubicin on A549 cells, vasculogenic mimicry (VM) channels and tumor metastasis. The enhanced antimetastatic mechanism of the targeted liposomes was attributed to the downregulation of matrix metalloproteinase-2 (MMP-2), vascular endothelial cadherin (VE-Cad), transforming growth factor- β 1 (TGF- β 1) and hypoxia inducible factor-1 α (HIF-1 α). Meanwhile, the targeted daunorubicin and dioscin codelivery liposomes exhibited significant antitumor effects in tumor-bearing mice. H&E staining, immunohistochemistry with Ki-67 and TUNEL assay also showed the promoted antitumor activity of the targeted liposomes.

Conclusion: Targeted daunorubicin and dioscin codelivery liposomes may provide an effective strategy for the treatment of NSCLC.

Keywords: daunorubicin, dioscin, liposomes, cell penetrating peptides, tumor metastasis, non-small-cell lung cancer

Introduction

Lung cancer is one of the most common malignancies worldwide.¹ It is the most common cause of cancer deaths among men and the second most common cause of cancer deaths among women.² According to its pathogenesis, lung cancer can be classified into small-cell lung cancer and non-small-cell lung cancer (NSCLC). NSCLC accounts for approximately 85% of all lung cancers and has a high level of tumor metastasis.³ At present, the treatments for NSCLC include surgery, chemotherapy, radiotherapy and immunotherapy.^{4,5} Among all the treatments, surgery is only performed for early stage lung cancer patients, and chemotherapy is the main therapy for NSCLC. However, the effects of conventional chemotherapy for

NSCLC remain poor due to the non-selectivity of chemotherapy drugs, the formation of vasculogenic mimicry (VM) channels and tumor cell metastasis. Therefore, it is urgent to develop a method for conventional chemotherapy to treat NSCLC by solving the problems listed above.

Tumor metastasis is a multistep process that includes tumor cells separating from the primary site, being transferred through lymphatic vessels or in the blood circulation, and finally reaching another distant organ to continue proliferation. It has been reported that tumor metastasis is the major reason for the failure of lung cancer therapy.⁶ Tumor metastasis is mainly related to the invasion and migration ability of tumor cells, the generation of VM channels and the expression of metastasis-related proteins, such as matrix metalloproteinase-2 (MMP-2), vascular endothelial cadherin (VE-Cad), transforming growth factor- β 1 (TGF- β 1) and hypoxia inducible factor-1 α (HIF-1 α).⁷

Daunorubicin is a clinically approved chemotherapeutic agent and is widely applied for many malignant tumors, including lung cancer. However, daunorubicin administered in its free form may have poor tumor selectivity and cause obvious side-effects, such as acute cardiotoxicity and bone marrow depression.⁸ The emergence of drug carriers has made up for the shortcomings of free drugs. Liposomes are one of the most promising drug delivery system which can encapsulate both hydrophilic drugs and hydrophobic drugs. The lipid bilayer of liposomes is composed of phospholipids and cholesterol, which are quite similar to the cell membrane. These liposomal features show an excellent biocompatibility compared to other drug carriers.⁹⁻¹¹ As a nanoscale drug carrier, liposomes can accumulate easily in tumor tissues due to the enhanced permeability and retention (EPR) effect and be targeted to tumor cells by their decoration with proteins, antibodies, aptamers or polypeptides.¹²⁻¹⁷

Cell penetrating peptides (CPPs) are polypeptide segments of various lengths that have the capacity to penetrate cellular membrane barriers.^{18,19} In recent years, CPPs have been successfully used to modify drug delivery carriers to facilitate their intracellular uptake.²⁰⁻²² Most CPPs are cationic, and this may induce systemic toxicity because of their positive charges. PFVYLI (PFV) is an electronically neutral cell penetrating peptide composed of six amino acids. It is a hydrophobic penetration peptide that has been shown to enhance the cellular uptake of drug delivery systems.²³⁻²⁵

Dioscin, a typical natural product, has been extracted from medicinal plants such as *Dioscorea nipponica*

Makino and *Dioscorea zingiberensis* Wright.^{26,27} Recently, evidence has shown that dioscin can inhibit tumor cell metastasis in lung cancer, breast cancer, melanoma and laryngeal cancer.²⁸⁻³² It has been proven that dioscin can suppress the invasion and migration of lung cancer cells.²⁹ To the best of our knowledge, there are no reports combining daunorubicin and dioscin to treat lung cancer by inhibiting tumor metastasis.

In the present study, a kind of targeted daunorubicin and dioscin codelivery liposomes was prepared to treat NSCLC by killing tumor cells and inhibiting tumor cell metastasis. In the targeted liposomes, PFV was modified on the liposomal surface to enhance active targeting, dioscin was encapsulated into the lipid bilayer to inhibit tumor metastasis, and daunorubicin was loaded into the hydrophilic part of the liposomes as an antitumor drug. The objectives of this paper were to develop targeted liposomes, evaluate their blocking effects and mechanism against tumor metastasis, and study their antitumor effects on metastatic NSCLC in vivo and in vitro.

Materials and methods

Materials and cells

Egg yolk phosphatidylcholine (EPC), cholesterol (Chol), and 1,2-distearoyl-sn-glycero-3-phosphoethanolamine-N [carboxy (polyethylene glycol)-2000] (DSPE-PEG₂₀₀₀-COOH) were obtained from the Avanti Polar Lipids, Inc. (Alabaster, AL, USA). Polyethylene glycol-distearoyl phosphatidylethanolamine (DSPE-PEG₂₀₀₀) was purchased from the NOF Corporation (Tokyo, Japan). Daunorubicin was supplied by the Meilun Biotechnology Co., Ltd. (Dalian, China). Dioscin was obtained from the Chengdu Derick Biotechnology Co., Ltd. (Chengdu, China). PFVYLI was synthesized by the GL Biochem Co., Ltd. (Shanghai, China). MMP-2, VE-Cad, TGF- β 1 and HIF-1 α enzyme-linked immunosorbent assay (ELISA) kits were ordered from the Lengton Bioscience Co., Ltd. (Shanghai, China). 4',6-diamidino-2-phenylindole (DAPI), Annexin V-FITC/PI apoptosis detection kit and reactive oxygen species (ROS) assay kit (DCFH-DA) were obtained from the Solarbio Science & Technology Co., Ltd. (Beijing, China). 1,1-dioctadecyl-3,3,3,3-tetramethylindotricarbocyanine iodide (DiR) and terminal deoxynucleotidyl transferase-mediated dUTP-biotin nick end labeling (TUNEL) kit were purchased from the Kaiji Biological Technology Development Co., Ltd. (Nanjing, China). Ki-67 antibody was provided by the Wanleibio Co., Ltd. (Shenyang, China). All other reagents were analytical grade.

A549 cells were purchased from the Institute of Basic Medical Science, Chinese Academy of Medical Science (Beijing, China). Cells were cultured in RPMI-1640 culture medium (Gibco) supplemented with 10% fetal bovine serum (Sijiqing, Hangzhou, China), 100 U/mL penicillin and 100 µg/mL streptomycin. The cell culture system was maintained at 37 °C in 5% CO₂. Male BALB/c nude mice of 18–20 g were obtained from the Peking University Experimental Animal Center (Beijing, China). All procedures were performed according to the guidelines of the Institutional Authority for Laboratory Animal Care of Peking University, and this research was approved by the Institutional Authority for Laboratory Animal Care of Peking University.

Synthesis of the targeting molecule

The targeting molecule, DSPE-PEG₂₀₀₀-PFV, was synthesized from DSPE-PEG₂₀₀₀-COOH and PFV peptide. In brief, DSPE-PEG₂₀₀₀-COOH was dissolved in DMF, and the solution was stirred for 1 h to activate carboxyl groups for reaction with EDC, NHS and DMAP. After adjusting the pH to 9 with N-methylmorpholine, PFV peptide was added to the solution at a molar ratio of 1:1 (DSPE-PEG₂₀₀₀-COOH:PFV). The reaction solution was stirred for 24 h at room temperature, and unbound materials were removed using a dialysis bag (MW cut-off, 3,000 Da). Then, the solution was lyophilized and characterized by matrix-assisted laser desorption/ionization time-of-flight mass spectrometry (MALDI-TOF-MS, Shimadzu, Japan) to verify the successful synthesis of DSPE-PEG₂₀₀₀-PFV.

Preparation of liposomes

Liposomes were prepared according to our previous report.^{33,34} Briefly, EPC, Chol, DSPE-PEG₂₀₀₀, DSPE-PEG₂₀₀₀-PFV and dioscin (100:30:3:2:7, molar ratio) were dissolved in chloroform in a round bottom flask. Then, the organic solvent was removed by a rotary evaporator at 40 °C to obtain a thin film. The lipid film was hydrated by sonication in a water bath for 5 min with 5 mL ammonium sulfate (250 mM), followed by sonification at 500 W for 10 min in an ice bath with a probe ultrasonicator. Subsequently, the suspension was extruded 3 times using a polycarbonate membrane with a pore size of 200 nm. Then, the targeted dioscin liposomes were obtained, and the prepared liposomes were sealed in a dialysis bag (MW cut-off, 8,000–14,000 Da) and dialyzed in phosphate buffered saline (PBS, 0.01 M, pH 7.4) for 24 h, followed by incubation with daunorubicin solution

(lipids:drug=100:7, molar ratio) in a water bath at 40 °C while shaking for 20 min. The targeted daunorubicin and dioscin codelivery liposomes were thus prepared.

Other liposomes were prepared according to the same procedures, and the compositions were as follow: EPC:Chol:DSPE-PEG₂₀₀₀:DSPE-PEG₂₀₀₀-PFV (100:30:3:2, molar ratios) for blank liposomes, EPC:Chol:DSPE-PEG₂₀₀₀:dioscin (100:30:5:7, molar ratios) for dioscin liposomes, EPC:Chol:DSPE-PEG₂₀₀₀:daunorubicin (100:30:5:7, molar ratios) for daunorubicin liposomes and EPC:Chol:DSPE-PEG₂₀₀₀:daunorubicin: dioscin (100:30:5:7:7, molar ratios) for daunorubicin and dioscin codelivery liposomes. In addition, DiR liposomes and targeted DiR liposomes were prepared in the same way (lipids:DiR=200:1, w/w) to evaluate targeting effects.

Characterization of liposomes

Particle size, polydispersity index (PDI) and zeta potential values of the liposomes were measured by dynamic light scattering (DLS, Zetasizer Nano ZS90 instrument, Malvern, UK). Each test was repeated three times. The morphology of the targeted daunorubicin and dioscin codelivery liposomes was observed by a transmission electron microscope (JEM-1200EX; JEOL, Tokyo, Japan) with an accelerating voltage of 120 kV and by atomic force microscopy (Cypher AFM, Asylum Research Inc, Santa Barbara, CA, USA) in tapping mode with a silicon probe (resonance frequency ~70 kHz, spring constants ~2 N/m).

To determine the encapsulation efficiency (EE) of the liposomes, unloaded daunorubicin and dioscin were separated from the original liposomes using a Sephadex G-50 column, and the purified liposomes were then ruptured with adequate methanol. The amount of daunorubicin and dioscin in the original liposomes and the eluted liposomes were quantified using high-performance liquid chromatography (HPLC, Shimadzu LC-20AT) at wavelengths of 233 nm and 203 nm, respectively. The mobile phases were acetonitrile/0.02mol/L sodium dihydrogen phosphate (32:68, v/v) for daunorubicin quantification and acetonitrile/water (65:35, v/v) for dioscin quantification. The EEs of drug-loaded liposomes were calculated using the following equation:

$$EE\% = \frac{\text{Amount of drug loaded in liposomes}}{\text{Amount of drug used for liposomal preparation}} \times 100\%$$

The in vitro release behavior of the daunorubicin liposomes, daunorubicin and dioscin codelivery liposomes,

targeted daunorubicin and dioscin codelivery liposomes was assessed by dialysis. Briefly, equal volumes of drug-loaded liposomes and PBS (1 mL) were placed in a dialysis bag (MW cut-off, 8,000–14,000 Da). The dialysis bag was immersed in 40 mL PBS and incubated in an orbital shaker at 100 rpm at 37 °C. At predetermined time intervals (12, 24, 36, 48, 60 and 72 h), 500 µL of the release medium was withdrawn, and replaced by the same volume of fresh PBS. The daunorubicin content in the release medium was determined by HPLC, and each assay was repeated in triplicate.

Optimum content of the targeting molecule

To confirm the optimum dosage of the targeting molecule, targeted daunorubicin liposomes consisting of different DSPE-PEG₂₀₀₀-PFV concentrations were used in a cellular uptake experiment. Briefly, A549 cells were grown in 6-well culture plates at a density of 2×10^5 cells per well. After being cultured for 24 h, the cells were treated with targeted daunorubicin liposomes with different concentrations of DSPE-PEG₂₀₀₀-PFV and incubated for different times (0.5, 1, 2 and 3 h). The amounts of DSPE-PEG₂₀₀₀-PFV in the targeted daunorubicin liposomes were 100:1, 100:2 and 100:4 (EPC:DSPE-PEG₂₀₀₀-PFV, molar ratio). Cells treated with daunorubicin liposomes were used as a control. The content of daunorubicin taken up in each group was measured by an Accuri C6 flow cytometer (Becton Dickinson, USA), and each assay was repeated in triplicate.

Cellular uptake and targeting effects in A549 cells

To investigate the cellular uptake, A549 cells were seeded in 6-well culture plates at a density of 2×10^5 cells per well for 24 h at 37 °C. Culture medium containing free daunorubicin, daunorubicin liposomes, daunorubicin and dioscin codelivery liposomes or targeted daunorubicin and dioscin codelivery liposomes was then added. The final daunorubicin concentration in each well was 35 µM. After incubation for 2 h, cells were washed with PBS three times, harvested and resuspended in 500 µL PBS. The cellular uptake was quantified using flow cytometry as mentioned above.

To observe intracellular targeting effects, A549 cells were grown at a density of 2×10^5 cells per well in 6-well plates for 24 h at 37 °C. Then, the cells were incubated

with free daunorubicin, daunorubicin liposomes, daunorubicin and dioscin codelivery liposomes or targeted daunorubicin and dioscin codelivery liposomes with a 35 µM final concentration of daunorubicin for 2 h. After incubation, the cells were washed with cold PBS, fixed with 4% (v/v) paraformaldehyde at room temperature for 15 min, and stained with DAPI for 5 min for cell nuclear staining. Finally, cells were imaged using a fluorescence microscope (Nikon Eclipse E800, Nikon, Tokyo).

Cytotoxicity assay

The cytotoxicity of the free drugs and the drug-loaded liposomes to A549 cells was measured by sulforhodamine B (SRB) assay. Briefly, A549 cells were seeded in 96-well plates at a density of 1×10^4 cells per well for 24 h at 37 °C. For the free drug groups, cells were treated with free dioscin, free daunorubicin or free daunorubicin and dioscin at different ratios. The concentration range for daunorubicin was 0–2.5 µM, and the ratios of daunorubicin to dioscin were 2:1, 1:1 and 1:2, respectively. For the liposomal groups, cells were exposed to blank liposomes, dioscin liposomes, daunorubicin liposomes, daunorubicin and dioscin codelivery liposomes or targeted daunorubicin and dioscin codelivery liposomes. The concentration range for both daunorubicin and dioscin was 0–10 µM (daunorubicin:dioscin=1:1, molar ratio). After 48 h of incubation, cells were fixed with 10% trichloroacetic acid at 4 °C and stained with 0.4% SRB. Stained cells were dissolved in Tris base solution, and the absorbance was measured using an enzyme-linked immunosorbent assay reader (HBS-1096A, DeTie, Nanjing, China) at 540 nm. The survival rates for A549 cells were calculated with the following formula: $\text{Survival\%} = (\text{A540 nm for treated cells} / \text{A540 nm for control cells}) \times 100\%$, where A540 nm represents the absorbance value at 540 nm.

Inhibition of VM formation

A Matrigel®-based tube formation assay was applied to assess the inhibition of VM channel formation in A549 cells. Briefly, Matrigel was placed into a 96-well plate (50 µL/well), and the plate was incubated at 37 °C for 30 min to solidify the Matrigel. A549 cells in serum-free culture medium were then seeded on the Matrigel at a density of 4×10^4 cells/well. Dioscin liposomes, daunorubicin liposomes, daunorubicin and dioscin codelivery liposomes or targeted daunorubicin and dioscin codelivery liposomes were added to the culture medium. Culture medium was used as blank control, and the final concentration of daunorubicin or dioscin was 10 µM. After 4 hrs

of incubation, the formation of VM channels was observed and photographed using an inverted microscope (XDS-1B, Chongqing Photoelectric Co., Ltd., Chongqing, China).

Blocking effects on wound healing and tumor migration

To determine the effects of the liposomes on invasion, a wound healing assay was carried out. Briefly, A549 cells were plated in 6-well plates (2×10^5 cells/well) and incubated overnight at 37 °C. When the cells reached approximately 80% confluence, a linear scratch was made through the cell monolayer with a sterile pipette tip. Then, the cells were washed with PBS solution three times, and the varying liposomal formulations were added to the medium with daunorubicin or dioscin at a final concentration of 10 μ M. Culture medium was used as blank control, and cells were cultured for 24 h at 37 °C. Images were taken 0, 12 and 24 h after scratching using an inverted microscope. Wound healing capacity was measured by the distance that cells spread from the leading edge of the wound.

A migration assay was performed in a Transwell chamber according to a previous report.³⁵ Briefly, 5×10^4 A549 cells in serum-free medium were seeded into the upper chamber of a Transwell insert, and 600 μ L of medium containing 5% serum was placed in the lower chamber. Then, cells in the upper chamber were treated with the varying drug-loaded liposomes with daunorubicin or dioscin at a final concentration of 10 μ M for 24 h. Culture medium was used as blank control. Subsequently, the upper chambers were washed with PBS, and non-migrated cells were removed with humid cotton. The migrated cells were fixed with 4% paraformaldehyde for 20 min, stained with 0.1% crystal violet for 30 min and washed with PBS 3 times. Migrated cells were observed and photographed using an inverted microscope.

Regulation of metastasis-related proteins

To study the inhibition mechanism of metastasis induced by drug-loaded liposomes, the concentrations of MMP-2, VE-Cad, TGF- β 1 and HIF-1 α were determined by ELISA. Briefly, A549 cells were cultured in a culture bottle. After reaching approximately 80% confluence, cells were treated with dioscin liposomes, daunorubicin liposomes, daunorubicin and dioscin codelivery liposomes or targeted daunorubicin and dioscin codelivery liposomes with daunorubicin or dioscin at a concentration of 10 μ M. Culture medium was used as blank control. After incubation for 12 h, cells were lysed, and the total proteins were collected by centrifugation. The concentrations

of metastasis-related proteins were determined according to the ELISA instructions, and the absorbance value of each protein was detected by a microplate reader at 450 nm. The total protein concentrations were measured at 540 nm by a bicinchoninic acid kit. The expression ratio was calculated using the following formula: expression ratio = (A450 nm for treated cells/A540 nm for treated cells)/(A450 nm for control cells/A540 nm for control cells), where A450 nm and A540 nm are the absorbance values at 450 and 540 nm, respectively. Each assay was repeated in triplicate.

Apoptotic effects on A549 cells

An Annexin V-FITC/PI kit was applied to evaluate the apoptotic effects on A549 cells after treatment with the varying liposomes. Briefly, A549 cells were seeded into 6-well plates at a density of 2×10^5 cells per well and incubated for 24 h. Then, cells were treated with dioscin liposomes, daunorubicin liposomes, daunorubicin and dioscin codelivery liposomes or targeted daunorubicin and dioscin codelivery liposomes for another 24 h. Culture medium was used as blank control, and the final concentration of daunorubicin or dioscin in the medium was 10 μ M. After that, cells were digested by trypsin without EDTA, collected by centrifugation and resuspended in binding buffer to a cell density of 1×10^6 cells/mL. The samples were stained with Annexin V-FITC and PI according to the manufacturer's instructions, and the number of apoptotic cells was determined by a flow cytometer. Each assay was repeated in triplicate.

To investigate the possible apoptosis mechanism induced by the liposomes, ROS level was measured by a ROS assay kit according to the previous research.³⁶ A549 cells were seeded into 6-well plates at a density of 2×10^5 cells per well and incubated for 24 h. Then, cells were treated with varying liposomal formulations and culture medium was used as blank control. The final concentration of daunorubicin or dioscin in medium was 10 μ M. After 24 h of incubation, DCFH-DA was added into the culture medium at a final concentration of 5 μ M and incubated with the cells for another 30 min before examining with fluorescence microscopy.

In vivo imaging and antitumor efficacy in tumor-bearing mice

A noninvasive optical imaging system was used to evaluate the targeting effects of the varying liposomes in vivo. Briefly,

BALB/c nude mice (16–18 g) were inoculated with A549 cells in the right flank by subcutaneous injection of 1×10^7 cells/200 μL culture medium. When the tumors reached approximately 400 mm^3 in volume, the tumor-bearing mice were randomly divided into four groups (3 mice per group). The mice were administered normal saline, free DiR, DiR liposomes or targeted DiR liposomes (2 μg DiR each) through the tail vein. Mice administered normal saline were used as blank control. After anesthetization with isoflurane, fluorescent images and X-ray images of the mice were captured using an in vivo imaging system (Carestream, FX Pro, USA) at 1, 2, 6, 12, 24 and 48 h.

To evaluate the pharmacodynamics of the varying liposomes, an A549 xenograft model was established as described above. When the tumors reached approximately 70 mm^3 in volume, all the mice were randomly divided into 6 groups ($n=8$) and administrated normal saline (blank control), free daunorubicin, dioscine liposomes, daunorubicin liposomes, daunorubicin and dioscine codelivery liposomes or targeted daunorubicin and dioscine codelivery liposomes every other day via tail vein injection 7 times. The concentrations of daunorubicin and dioscine administered were 5 mg/kg and 8 mg/kg , respectively. Tumor volume was determined using a vernier caliper and calculated by the following formula: $V (\text{mm}^3) = \text{length} \times \text{width}^2/2$. Tumor volume ratios were calculated with the following formula: $R = \text{tumor volume measured at the } n\text{th day} / \text{tumor volume measured at day 0}$. The body weights of the tumor-bearing mice were measured 7 times to evaluate the primary safety of the drugs. On the second day of the last administration, the mice were sacrificed by dislocation. The tumors were separated, embedded in paraffin and sliced into 5.0 μm sections for the subsequent assays. After 4 injections, 20 μL of blood was collected from the eye socket and used to examine hematological parameters using a hematology analyzer (MEK-6318K, Nihon, Kohden, Japan).

Hematoxylin and eosin (H&E) staining was applied to detect histopathological changes in the tumor tissues in each group. The stained sections were observed with an optical microscope. Tumor tissue proliferation was detected by immunohistochemistry with the Ki-67 antibody. Briefly, tumor sections from the varying groups were incubated with the Ki-67 antibody (1:300) at 4 $^{\circ}\text{C}$ overnight. After washing with PBS three times, the sections were incubated with secondary antibody (1:500) for 1 h. The results were observed and photographed by an inverted microscope using DAB as a chromogenic reagent. To detect apoptotic cells in tumor tissues, a TUNEL immunofluorescence kit was used according to the manufacturer's protocol. Then, the cell nuclei were

stained with DAPI, and the tumor slides were imaged under a fluorescence microscope.

Statistical analysis

One-way ANOVA was used for comparison of the results. The results are presented as the mean \pm SD of at least three samples, and $p < 0.05$ was considered to be significant.

Results

Synthesis of the targeting molecule

The MALDI-TOF-MS spectrum of the targeting molecule is shown in Figure 2A. The average masses of DSPE-PEG₂₀₀₀-COOH and DSPE-PEG₂₀₀₀-PFV were 2,994.15 (Figure 2A1) and 3,711.39 (Figure 2A2), respectively. The mass difference between the two molecules corresponded to the mass of PFV. The MALDI-TOF-MS spectrum results verified the successful synthesis of DSPE-PEG₂₀₀₀-PFV.

Characterization of the liposomes

A schematic illustration of the targeted daunorubicin and dioscine codelivery liposomes is shown in Figure 1. Physical properties including particle size, polydispersity index (PDI), zeta potential and EE are listed in Table 1. The results showed that the average particle size of the targeted daunorubicin and dioscine codelivery liposomes was 121.13 ± 1.58 nm, and the targeted liposomes exhibited a narrow PDI (approximately 0.2) and a relatively stable zeta potential of -10.4 ± 0.25 mV. As shown in Table 1, the EEs for daunorubicin and dioscine in the targeted liposomes were $93.78 \pm 0.75\%$ and $91.46 \pm 5.40\%$, respectively. TEM (Figure 2B) and AFM images (Figure 2D) showed that the targeted daunorubicin and dioscine codelivery liposomes were nearly spherical. An in vitro release experiment indicated that all the liposomes exhibited sustained release. For the targeted daunorubicin and dioscine codelivery liposomes, the release rate was approximately 50% at 37 $^{\circ}\text{C}$ after 72 h (Figure 2C).

Optimum concentration of the targeting molecule

To confirm the optimum concentration of the targeting molecule, the cellular uptake of liposomes with different PFV concentration was measured by flow cytometry. As shown in Figure 3A, the fluorescence intensity was enhanced with the increasing addition of PFV and with increasing time. Compared with the third group (EPC:DSPE-PEG₂₀₀₀-

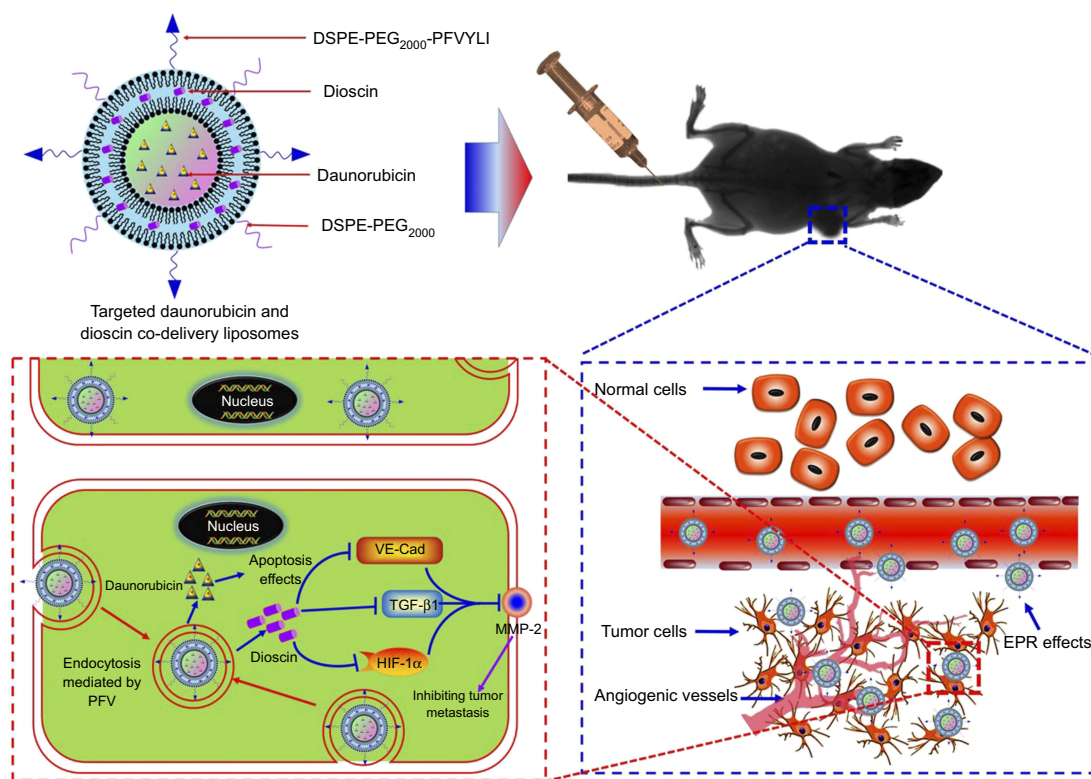


Figure 1 Schematic illustration of strategy of inhibiting tumor metastasis by targeted daunorubicin and dioscin codelivery liposomes.

Abbreviations: PFV, PFVYLI; DSPE-PEG₂₀₀₀, polyethylene glycol-distearoyl phosphatidylethanolamine; EPR effect, enhanced permeability and retention effect; VE-Cad, vascular endothelial cadherin; TGF- β 1, transforming growth factor- β 1; HIF-1 α , hypoxia inducible factor-1 α ; MMP-2, matrix metalloproteinase-2.

Table 1 Particle size, zeta potential and encapsulation efficiency of liposomes

Liposomes	Size (nm)	PDI	Zeta (mV)	EE%	
				Daunorubicin	Dioscin
Blank liposomes	93.71 \pm 1.14	0.152 \pm 0.002	-13.7 \pm 0.47	—	—
Dioscin liposomes	108.67 \pm 0.84	0.212 \pm 0.010	-15.2 \pm 0.47	—	93.60 \pm 1.65
Daunorubicin liposomes	96.9 \pm 2.80	0.134 \pm 0.020	-13.2 \pm 0.33	94.31 \pm 0.81	—
Daunorubicin and dioscin codelivery liposomes	118.17 \pm 1.51	0.230 \pm 0.025	-10.9 \pm 0.78	92.80 \pm 0.80	92.12 \pm 6.43
Targeted daunorubicin and dioscin codelivery liposomes	121.13 \pm 1.58	0.245 \pm 0.024	-10.4 \pm 0.25	93.78 \pm 0.75	91.46 \pm 5.40

Note: Data are presented as mean \pm SD (n=3).

Abbreviations: PDI, polydispersity index; EE, encapsulation efficiency.

PFV=100:2), the fluorescence intensity in the fourth group (EPC:DSPE-PEG₂₀₀₀-PFV=100:4) was not significantly increased. Hence, the ratio of EPC to DSPE-PEG₂₀₀₀-PFV used was 100:2.

Cellular uptake and targeting effects in A549 cells

The cellular uptake of the varying formulations was determined by flow cytometry, and photographed by fluorescence microscopy. Quantitative analysis of cellular uptake is shown

in Figure 3B. The fluorescence intensity of the targeted daunorubicin and dioscin codelivery liposomes was higher than that of the other two liposomal groups, and free daunorubicin showed the highest fluorescence intensity for the direct contact with tumor cells. Images showing the cellular internalization of daunorubicin are shown in Figure 3C. In the merged channels, the targeted daunorubicin and dioscin codelivery liposomes exhibited higher intracellular fluorescence than the other liposomal groups. The intracellular fluorescence results were consistent with the results from flow cytometry experiments.

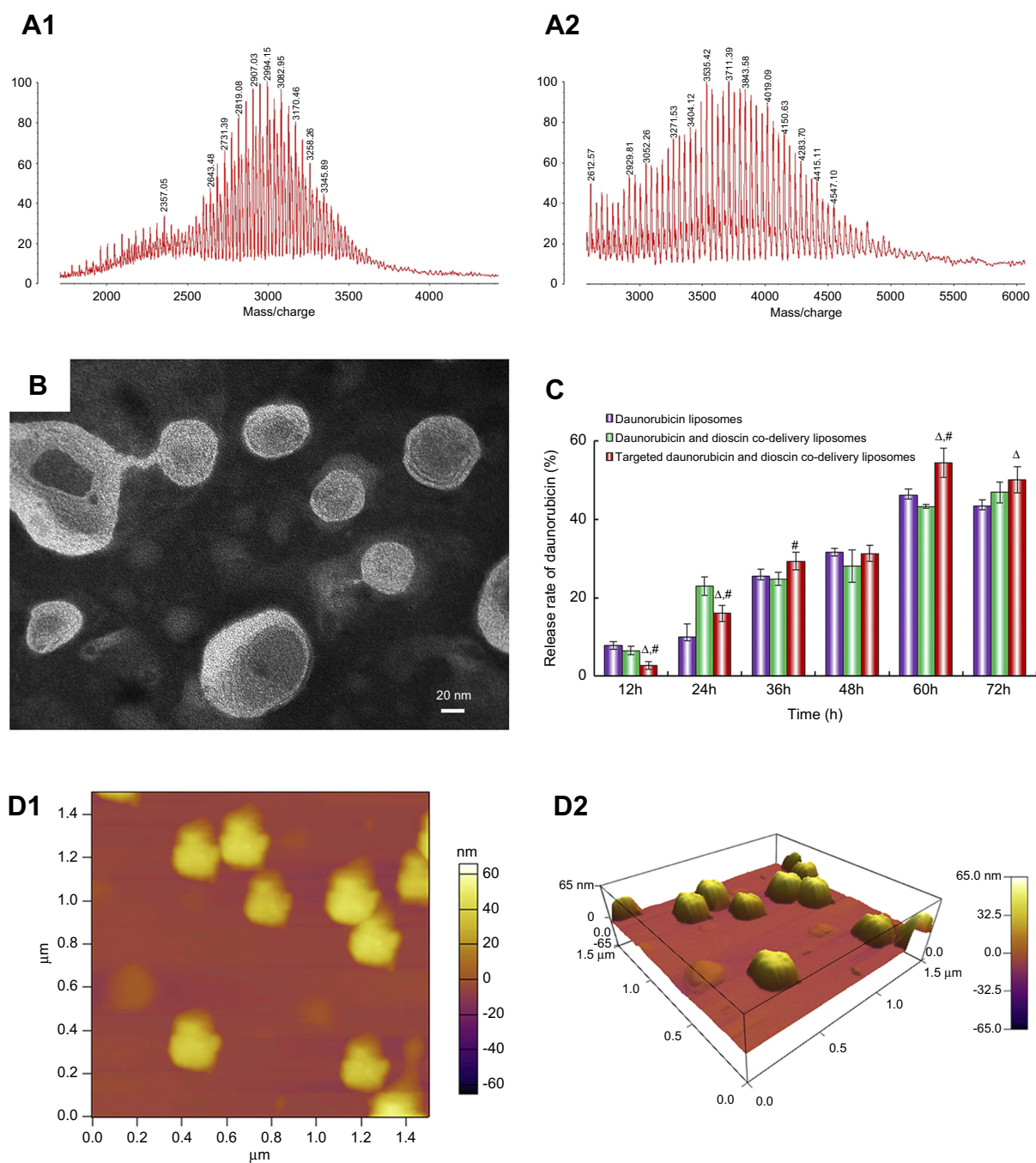


Figure 2 Characterization of liposomes. **(A1)** MALDI-TOF-MS spectrum of DSPE-PEG₂₀₀₀-COOH, **(A2)** MALDI-TOF-MS spectrum of DSPE-PEG₂₀₀₀-PFV, **(B)** TEM image of targeted daunorubicin and dioscine codelivery liposomes, **(C)** In vitro cumulative release profile of daunorubicin from varying liposomal formulations. Data are presented as mean \pm SD (n=3). Δ , vs Daunorubicin liposomes; #, vs Daunorubicin and dioscine codelivery liposomes. $p < 0.05$, **(D1)** AFM image of targeted daunorubicin and dioscine codelivery liposomes, **(D2)** 3D structure of **(D1)**.

Abbreviations: PFV, PFVYL; DSPE-PEG₂₀₀₀-COOH, 1,2-distearoyl-sn-glycero-3-phosphoethanolamine-N [carboxy (polyethylene glycol)-2000]; MALDI-TOF-MS, matrix-assisted laser desorption/ionization time-of-flight mass spectrometry; TEM, transmission electron microscope; AFM, atomic force microscope.

Cytotoxic effects

The cytotoxic effects of the varying formulations on A549 cells are shown in Figure 4. The results showed that free dioscine exerted almost no cytotoxicity on A549 cells at the tested concentrations. The cytotoxic effect of free

daunorubicin was enhanced with the addition of dioscine (Figure 4A). The IC₅₀ values were 0.89 \pm 0.14 μ M for free daunorubicin, 0.58 \pm 0.10 μ M for free daunorubicin and free dioscine (2:1, molar ratio), 0.27 \pm 0.06 μ M for free daunorubicin and free dioscine (1:1, molar ratio), 0.16 \pm 0.03 μ M for free

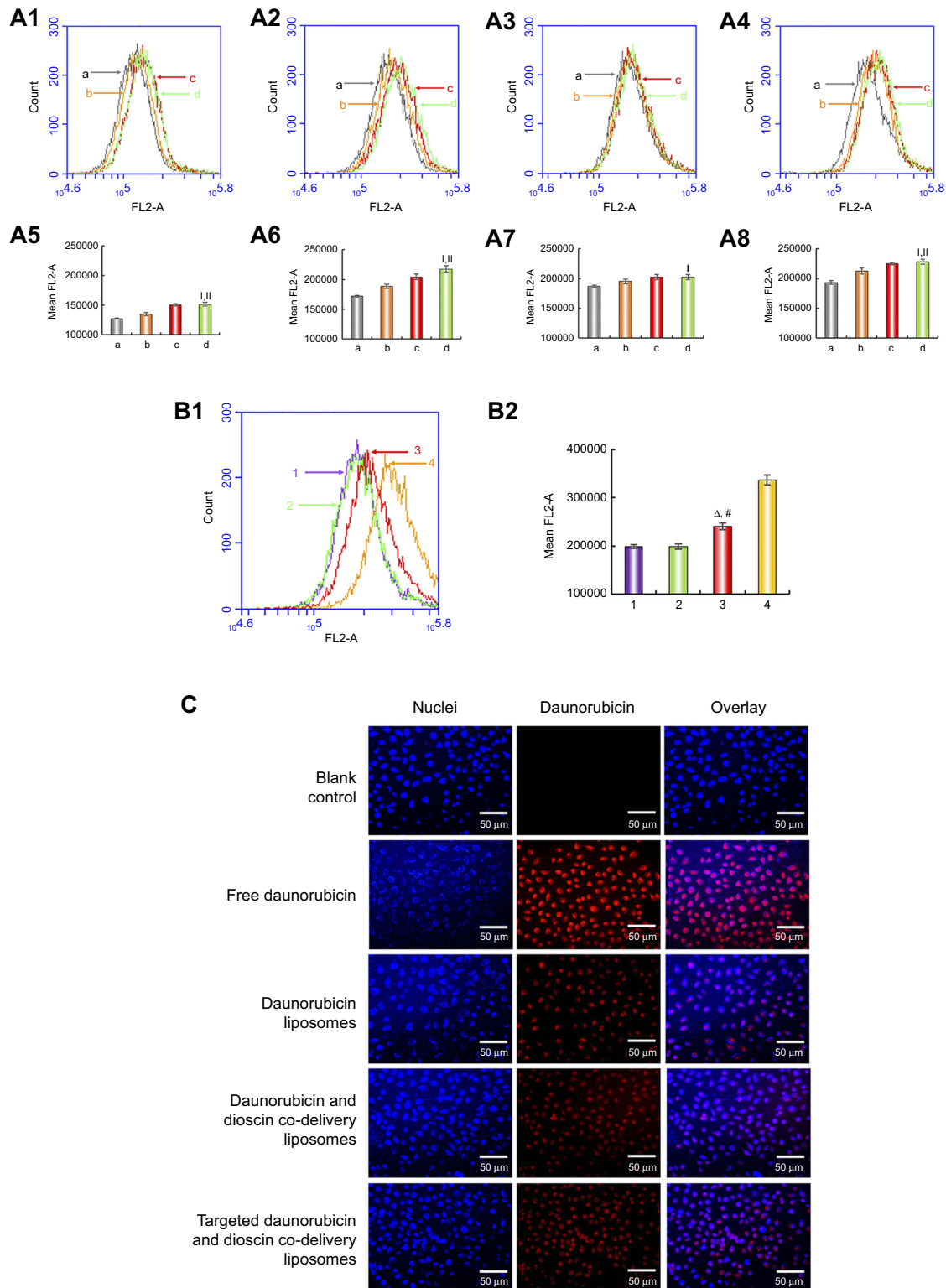


Figure 3 Cellular uptake and targeting effects after incubation with the varying formulations. **(A1)** Cellular uptake of A549 cells treated with targeted daunorubicin liposomes consist varying content of PFV for 0.5 h, **(A2)** Cellular uptake of A549 cells treated with targeted daunorubicin liposomes consist varying content of PFV for 1 h, **(A3)** Cellular uptake of A549 cells treated with targeted daunorubicin liposomes consist varying content of PFV for 2 h, **(A4)** Cellular uptake of A549 cells treated with targeted daunorubicin liposomes consist varying content of PFV for 3 h, **(A5)** Fluorescence intensity of (A1), **(A6)** Fluorescence intensity of (A2), **(A7)** Fluorescence intensity of (A3), **(A8)** Fluorescence intensity of (A4). a, EPC:DSPE-PEG₂₀₀₀-PFV=100:0; b, EPC:DSPE-PEG₂₀₀₀-PFV=100:1; c, EPC:DSPE-PEG₂₀₀₀-PFV=100:2; d, EPC:DSPE-PEG₂₀₀₀-PFV=100:4. Data are presented as mean \pm SD (n=3). I, vs a; II, vs b. $p < 0.05$. **(B1)** Cellular uptake of A549 cells treated with varying liposomal formulations or free drug, **(B2)** Fluorescence intensity of (B1). I, Daunorubicin liposomes; 2, Daunorubicin and dioscin codelivery liposomes; 3, Targeted daunorubicin and dioscin codelivery liposomes; 4, Free daunorubicin. Δ , vs Daunorubicin liposomes; #, vs Daunorubicin and dioscin codelivery liposomes. $p < 0.05$. **(C)** Fluorescence microscopy images of A549 cells incubated with the varying formulations.

Abbreviations: EPC, egg yolk phosphatidylcholine; PFV, PFVYLI.

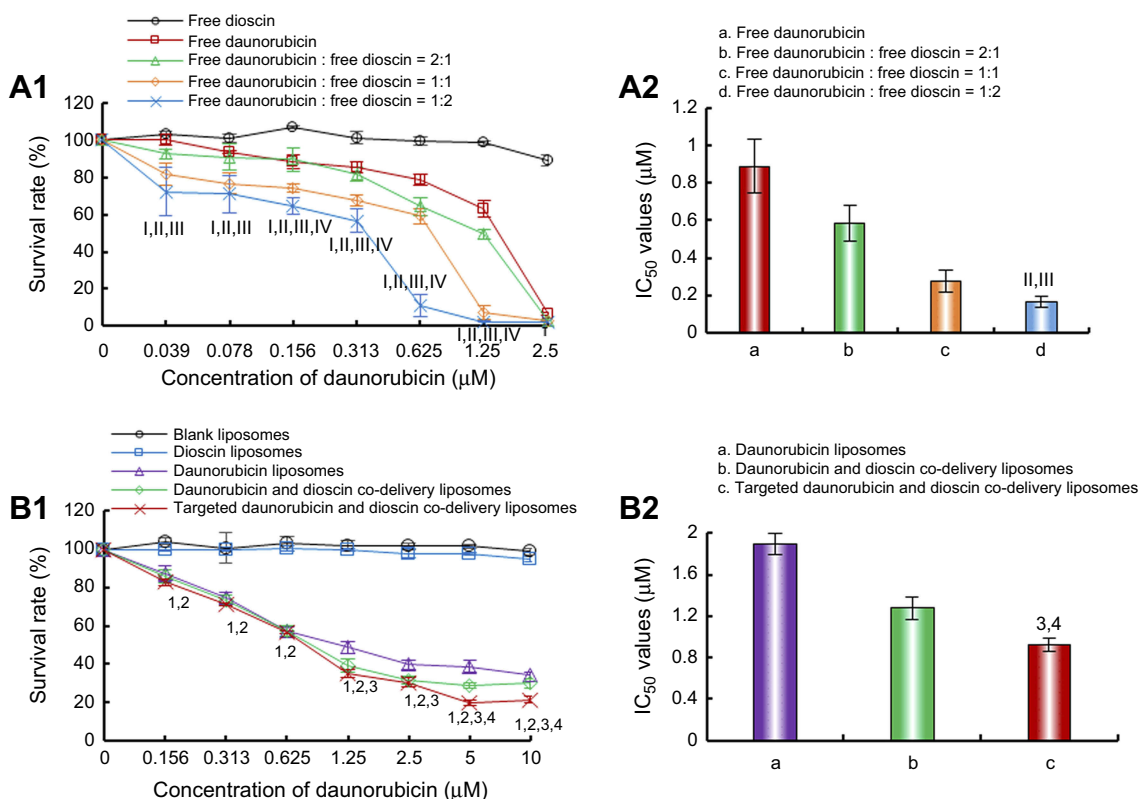


Figure 4 Inhibitory effects on A549 cells after treatments with the varying formulations. (A) Inhibitory effects of free drugs. I, vs Free dioscin; II, vs Free daunorubicin; III, vs Free daunorubicin : free dioscin=2:1; IV, vs Free daunorubicin : free dioscin=1:1; (B) Inhibitory effects of liposomal formulations. I, vs Blank liposomes; 2, vs Dioscin liposomes; 3, vs Daunorubicin liposomes; 4, vs Daunorubicin and dioscin codelivery liposomes. Data are presented as mean \pm SD (n=6). $p < 0.05$.

daunorubicin and free dioscin (1:2, molar ratio), respectively. Figure 4B shows the cytotoxicity of the varying liposomal formulations. Blank liposomes showed no cytotoxicity, which verified the safety of our materials. Dioscin liposomes showed nearly no cytotoxicity at the maximum concentration tested. The targeted daunorubicin and dioscin codelivery liposomes exhibited the strongest cytotoxic effects among all liposomal formulations. The IC_{50} values were $1.89 \pm 0.11 \mu\text{M}$, $1.27 \pm 0.11 \mu\text{M}$, $0.85 \pm 0.06 \mu\text{M}$ for daunorubicin liposomes, daunorubicin and dioscin codelivery liposomes, targeted daunorubicin and dioscin codelivery liposomes, respectively.

Inhibition of VM formation

Figure 5A describes the inhibitory effects on VM channels treated with varying liposomal formulations. After incubation for 4 h, vessel-like loops, networks and channels formed by A549 cells could be seen on the Matrigel for the control group. Daunorubicin liposomes showed slight inhibition of VM channel formation, and dioscin liposomes caused visible damage to the VM channels. Out of all the liposomal formulations, both daunorubicin and

dioscin codelivery liposomes and targeted daunorubicin and dioscin codelivery liposomes showed prominent inhibitory effects on VM channels.

Blocking effects on wound healing and tumor migration

Figure 5B shows the blocking effects of the varying liposomal formulations on wound healing. After incubation for 24 h, the scratch in the control group was almost healed. Compared with the control group, the mobility and invasion of A549 cells were significantly blocked in the liposome-treated groups.

The migration ability of A549 cells treated with the varying liposomal formulations was also examined by Transwell assay, and the results are shown in Figure 5C. For the control group, A549 cells exhibited strong transfer ability. Compared with the control group, daunorubicin and dioscin codelivery liposomes, targeted daunorubicin and dioscin codelivery liposomes showed stronger blocking effects on tumor cell migration.

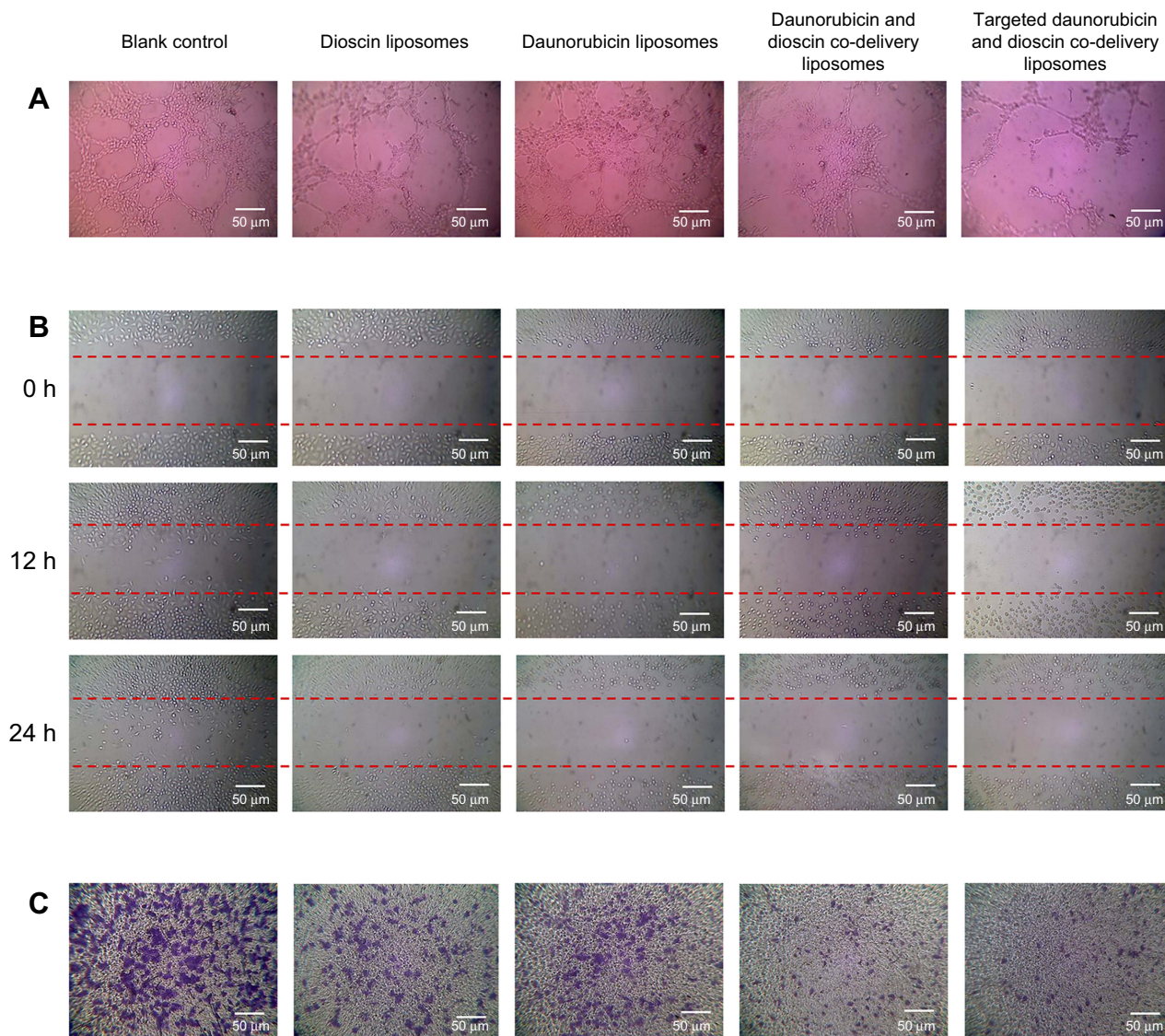


Figure 5 Inhibition of VM formation, wound healing and tumor migration. (A) Inhibition of VM formation, (B) Blocking effects on wound healing, (C) Blocking effects on tumor migration.

Abbreviation: VM, vasculogenic mimicry.

Regulating effects on metastasis-related proteins

To elucidate the mechanism of metastasis inhibition, the expression levels of four metastasis-related proteins, MMP-2, VE-Cad, TGF- β 1 and HIF-1 α , were determined by ELISA. The relative protein expression level ratios are shown in Figure 6. Compared with those in the control group, the expression levels of MMP-2, VE-Cad, TGF- β 1 and HIF-1 α were obviously reduced after treatment with the varying liposomal

formulations. The targeted daunorubicin and dioscin codelivery liposomes showed the strongest effect on metastasis-related proteins among all the groups. For the targeted daunorubicin and dioscin codelivery liposomes, the ratios between expression following liposomal treatment and expression without liposomal treatment were 0.35 ± 0.03 for MMP-2, 0.24 ± 0.13 for VE-Cad, 0.17 ± 0.04 for TGF- β 1 and 0.09 ± 0.01 for HIF-1 α .

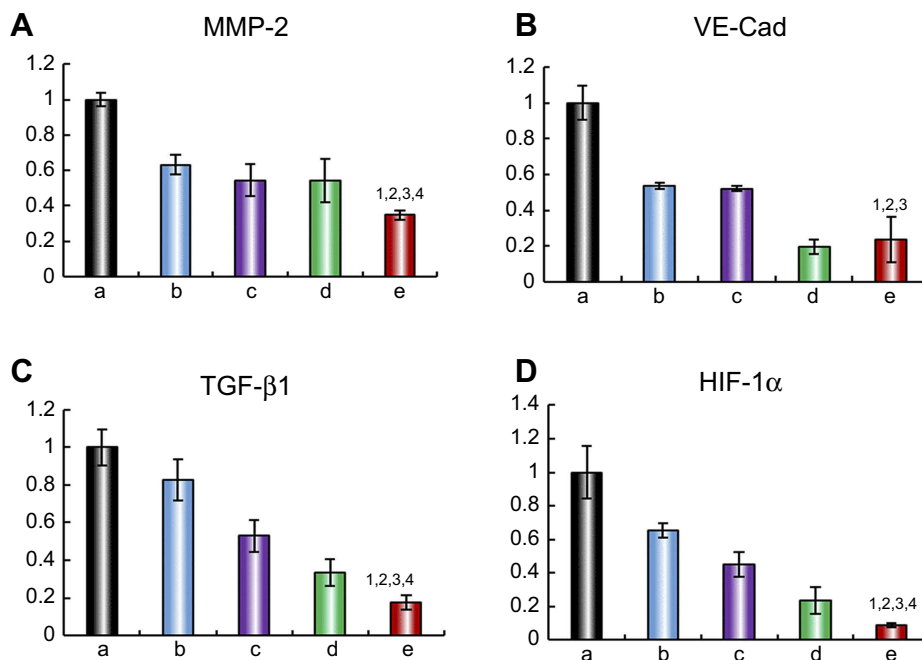


Figure 6 Regulating effects on metastasis-related proteins. (A) MMP-2 protein expression ratio, (B) VE-Cad protein expression ratio, (C) TGF-β1 protein expression ratio, (D) HIF-1α protein expression ratio. Data are presented as mean ± SD (n=3). a. Blank control; b. Dioscin liposomes; c. Daunorubicin liposomes; d. Daunorubicin and dioscin codelivery liposomes; e. Targeted daunorubicin and dioscin codelivery liposomes. 1, vs a; 2, vs b; 3, vs c; 4, vs d. $p < 0.05$.

Abbreviations: MMP-2, matrix metalloproteinase-2; VE-Cad, vascular endothelial cadherin; TGF-β1, transforming growth factor-β1; HIF-1α, hypoxia inducible factor-1α.

Apoptotic effects on A549 cells

Apoptosis was detected with flow cytometry after treatment with the varying liposomal formulations. As shown in Figure 7A, the lower left, lower right, and upper right quadrants represented viable, early apoptotic, and late apoptotic/necrotic regions, respectively.³⁷ The results showed that there was almost no apoptosis in the control group. The apoptosis rates of A549 cells treated with dioscin liposomes, daunorubicin liposomes, daunorubicin and dioscin codelivery liposomes, targeted daunorubicin and dioscin codelivery liposomes increased sequentially (Figure 7A). Out of all the liposomal formulations, the targeted daunorubicin and dioscin codelivery liposomes had the strongest apoptotic effect on A549 cells and caused approximately 40% of the cells to undergo apoptosis. The proportion of apoptosis after varying liposomal formulations treatment is shown in Figure 7B. The apoptosis induced by liposomes is closely related to the production of ROS. As shown in Figure 7C, compared to the control group, targeted daunorubicin and dioscin codelivery liposomes exhibited the highest fluorescence intensity, which indicated the highest ROS level in this group.

In vivo imaging and antitumor efficacy in tumor-bearing mice

Figure 8 shows the distribution of DiR in tumor-bearing mice after intravenous injection of the varying formulations. Compared with the free DiR group, both DiR liposomes and targeted DiR liposomes exhibited stronger tumor targeting capacity. Fluorescence from DiR could still be observed after liposome administration for 48 h in the liposomal groups, which indicated that liposomes had longer retention times in vivo. Meanwhile, the fluorescent signal of the targeted DiR liposomes was stronger than that of the DiR liposomes at the different time points.

Figure 9 shows the pharmacodynamics of the varying drug formulations. Except for the free daunorubicin group, the body weights of mice in all the groups showed no obvious decline during the administration (Figure 9A). Compared with the normal saline-treated group, all the drug-treated groups showed different degrees of tumor growth inhibition. Targeted daunorubicin and dioscin codelivery liposomes showed an obvious antitumor effect from the fourth day after the start of administration (Figure 9B). The hematological parameters are listed in Table 2. The administration of targeted daunorubicin and dioscin codelivery liposomes resulted in negligible changes in

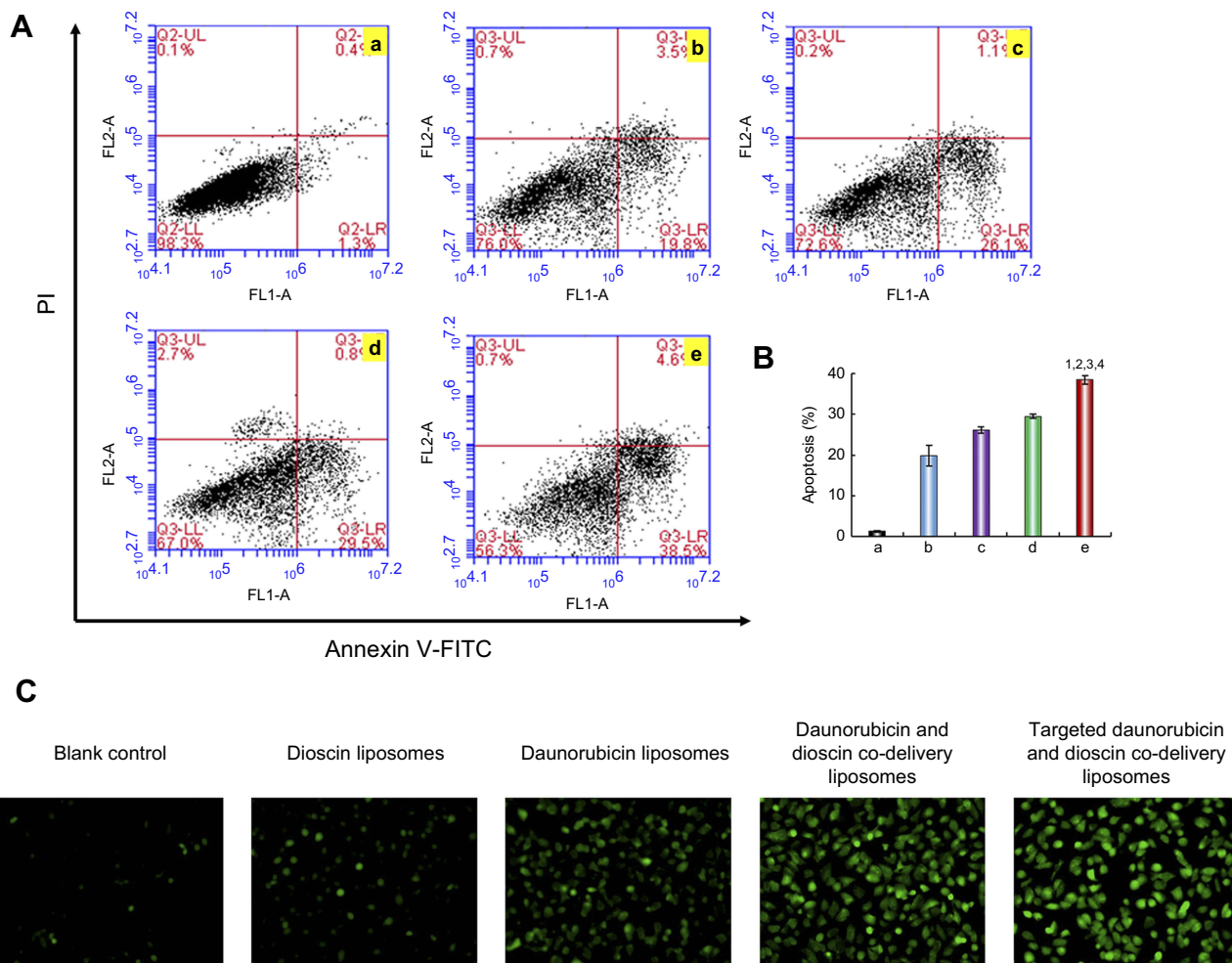


Figure 7 Apoptotic effects to A549 cells. (A) Apoptosis determined by flow cytometry, (B) The proportion of apoptosis after varying liposomal formulations treatment. Data are presented as mean \pm SD (n=3). a. Blank control; b. Dioscin liposomes; c. Daunorubicin liposomes; d. Daunorubicin and dioscine codelivery liposomes; e. Targeted daunorubicin and dioscine codelivery liposomes. 1, vs a; 2, vs b; 3, vs c; 4, vs d. $p < 0.05$. (C) Fluorescence microscopy images of intracellular ROS level in A549 cells. **Abbreviation:** ROS, reactive oxygen species.

hematological parameters compared with those observed in the normal saline-treated group.

H&E staining of tumor tissue sections showed increased necrotic or apoptotic cells after treatment with the targeted daunorubicin and dioscine codelivery liposomes (Figure 9C). Images showing immunohistochemical staining with Ki-67 are shown in Figure 9D. The results showed that the largest number of Ki-67-positive cells was in the normal saline-treated group. However, the number of Ki-67-positive cells reduced after treatment with the targeted daunorubicin and dioscine codelivery liposomes. To detect apoptotic cells in tumor tissues, a TUNEL assay was performed. As shown in Figure 9E, tumor tissues treated with targeted daunorubicin and dioscine codelivery liposomes exhibited the highest signal in the TUNEL assay, and fewer apoptotic cells were found in the

other groups. This result was consistent with the trend in apoptosis detected by flow cytometry in vitro.

Discussion

Chemotherapy for NSCLC treatment still faces poor clinical prognosis. The major obstacles for NSCLC treatment are tumor metastasis and the non-selectivity of chemotherapy drugs in vivo. The appearance of liposomal technology in recent years has provided a promising strategy for tumor-targeted drug delivery. Therefore, we developed targeted daunorubicin and dioscine codelivery liposomes to treat NSCLC by increasing active targeting and inhibiting tumor metastasis.

In this study, targeted daunorubicin and dioscine codelivery liposomes were successfully prepared by film

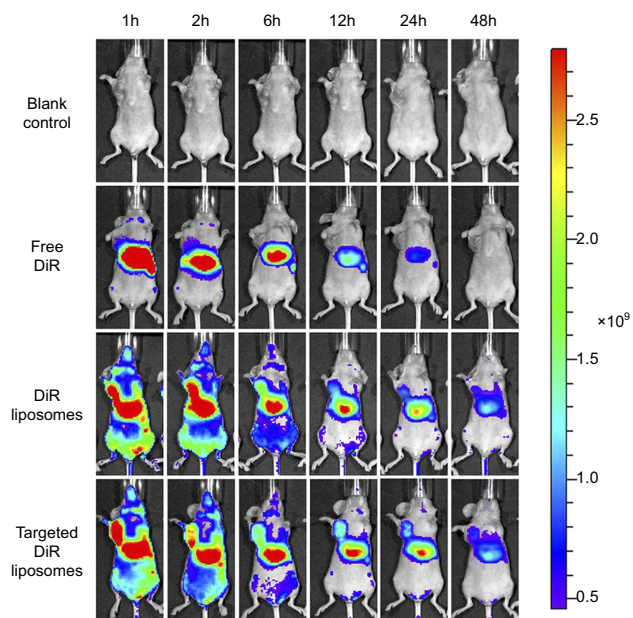


Figure 8 In vivo imaging in mice.

Abbreviation: DiR, 1,1-dioctadecyl-3,3,3,3-tetramethylindotricarbocyanine iodide.

dispersion and the ammonium sulfate gradient method. The targeted daunorubicin and dioscine codelivery liposomes exhibited satisfactory physicochemical characteristics: an average size of approximately 100 nm, a narrow polydispersity index, a relatively stable zeta potential and a higher encapsulation efficiency for both daunorubicin and dioscine (more than 90%). The particle size and zeta potential did not change greatly after modification with the PFV peptide (listed in Table 1). It is well known that liposomes approximately 100 nm in size can easily accumulate in tumor tissues due to the EPR effect.^{38,39} Therefore, the size of the targeted daunorubicin and dioscine codelivery liposomes was beneficial for tumor targeting. The diameter of the liposomes observed by AFM was slightly larger than that determined by DLS, which could be explained by the relatively flexible spread of liposomes on the mica surface.⁴⁰ Targeted daunorubicin and dioscine codelivery liposomes exhibited controlled release behavior, which could prolong their circulation time in the blood (Figure 2C).

The PFV peptide was successfully conjugated to DSPE-PEG₂₀₀₀-COOH, and the MALDI-TOF-MS spectra are shown in Figure 2A. To investigate the influence of DSPE-PEG₂₀₀₀-PFV density on cellular uptake, a series of targeted daunorubicin liposomes consisting of various DSPE-PEG₂₀₀₀-PFV concentrations were added to A549 cells, and the fluorescence intensity was measured by flow cytometry. Cellular uptake was enhanced with the

increasing addition of the targeting molecule. The ratio of group c was the final ratio used for liposome preparation because there was no significant difference between the fluorescence intensity for group c and group d (Figure 3A).

Flow cytometry and fluorescence microscopy were used with the cellular uptake assay to determine the targeting effects of the varying formulations. Flow cytometry result showed the intracellular fluorescence intensity was the highest after treatment with the targeted daunorubicin and dioscine codelivery liposomes among all liposomal formulations (Figure 3B). To obtain direct and visible evidence, cellular uptake was further evaluated by a fluorescence microscope (Figure 3C). The A549 cell nuclei were stained with DAPI and is shown in blue, and daunorubicin is shown in red. Bright blue/red spots represent the overlay of the fluorescent signals for daunorubicin and the nuclei. The results showed that targeted daunorubicin and dioscine codelivery liposomes had a higher intracellular fluorescence than the other two liposomes. These results from the cellular uptake experiments indicated that the modification of the liposomal surface with PFV could distinctly increase cellular uptake via increasing penetration of the cell membrane.

Cytotoxicity assays were performed to evaluate the inhibitory effects of free drugs and varying liposomal formulations on A549 cells. In the free drug-treated groups, the results indicated that the combination of daunorubicin with different concentrations of dioscine showed enhanced inhibitory effects on A549 cells compared with daunorubicin alone, and dioscine alone had negligible effects on the survival rate of A549 cells (Figure 4A), which demonstrated that dioscine enhanced the cytotoxicity of daunorubicin. In addition, the cytotoxicity of liposomes to A549 cells was further evaluated (Figure 4B). The IC₅₀ values for the varying liposomal formulations were different, which was mainly attributed to the addition of dioscine or PFV to the liposomes. This further confirmed that modification with PFV and the addition of dioscine could increase the active targeting and cytotoxicity of daunorubicin-containing liposomes to A549 cells.

Metastasis is the leading cause for tumor recurrence and death. Tumor metastasis is a complicated process and includes the formation of VM channels, invasion into adjacent tissue and migration to distant tissues.⁴¹

VM channels, which were first proposed in 1999, are usually generated by tumor cells under hypoxia to provide adequate nutrition for the rapid growth of tumors before

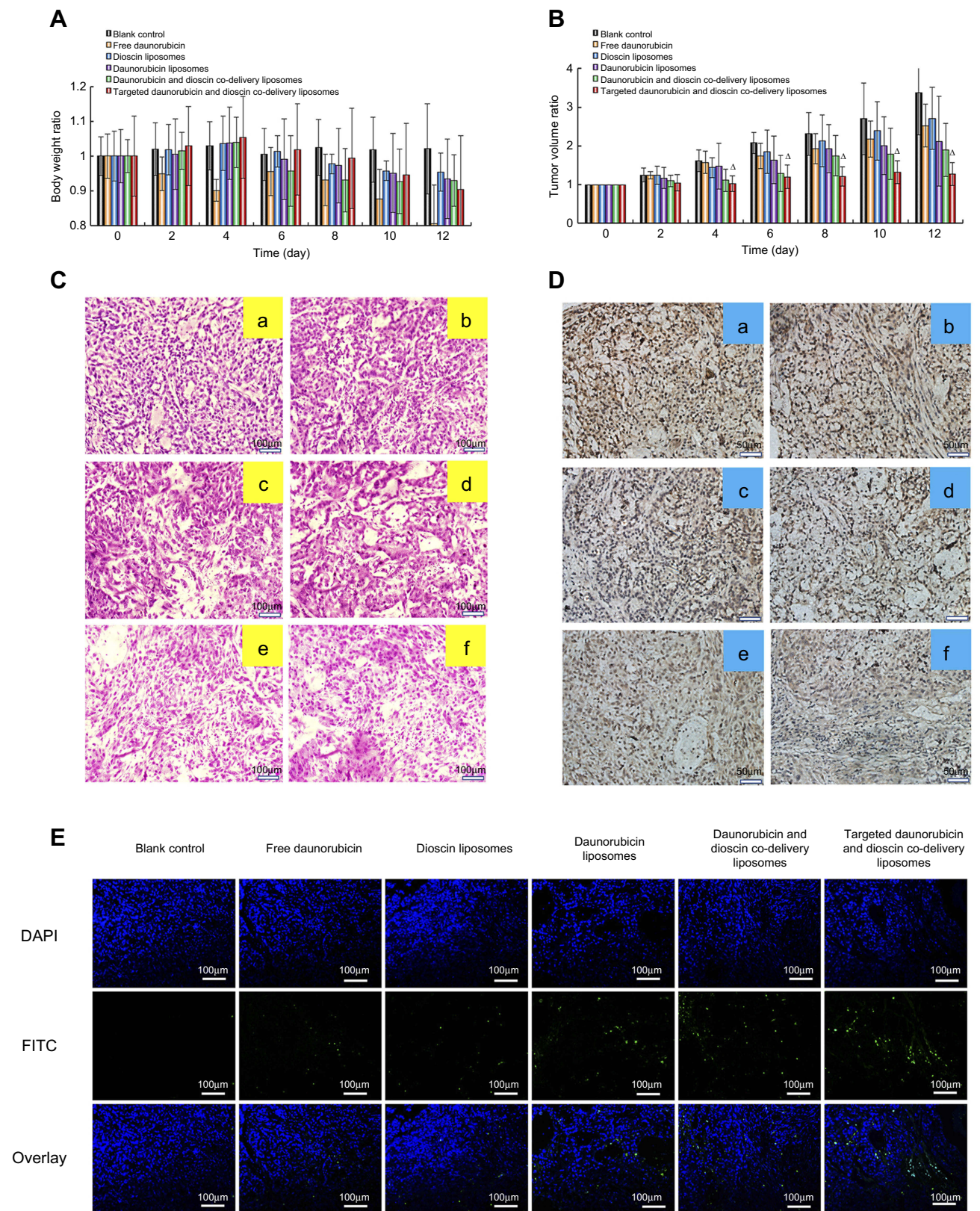


Figure 9 In vivo antitumor efficacy in tumor-bearing mice. (A) Body weight changes, (B) Tumor volume changes. Δ , vs Blank control, $p < 0.05$, (C) H&E staining assay, (D) Immunohistochemistry staining of the proliferation marker Ki-67 in tumor tissues. a, Blank control; b, Free daunorubicin; c, Dioscin liposomes; d, Daunorubicin liposomes; e, Daunorubicin and dioscin codelivery liposomes; f, Targeted daunorubicin and dioscin codelivery liposomes, (E) TUNEL assay for apoptotic cells.

Table 2 Hematology parameters assay results from tumor-bearing mice

Assay	Blank control	Free daunorubicin	Dioscin liposomes	Daunorubicin liposomes	Daunorubicin and dioscincodelivery liposomes	Targeted daunorubicin and dioscincodelivery liposomes
WBC	7.87±2.37	3.93±0.75	7.30±2.00	5.10±1.85	5.37±0.90	5.53±1.17
RBC	7.92±0.48	7.40±1.12	7.44±0.49	7.01±0.55	7.05±0.32	7.26±1.18
HGB	119.67±4.62	114.67±17.16	115.67±6.35	111.00±8.19	113.67±4.16	112.00±14.73
HCT	36.17±2.12	32.77±5.88	34.37±1.95	33.23±2.84	34.00±1.39	33.73±5.20
MCV	45.70±0.66	44.20±1.60	46.23±1.50	47.43±0.32	48.20±0.26	46.53±0.60
MCH	15.13±0.31	15.50±0.00	15.60±0.60	15.87±0.12	16.13±0.29	15.50±0.62
MCHC	331.00±6.56	351.33±13.50	336.33±2.52	334.33±4.16	334.33±3.79	332.67±10.21
RDW	16.63±1.40	17.23±1.78	16.17±1.37	15.17±2.25	14.30±1.60	14.63±0.75
PLT	585.33±29.28	586.33±148.18	601.67±27.54	567.00±49.73	577.00±68.09	738.33±150.39
PCT	0.22±0.01	0.22±0.04	0.22±0.03	0.20±0.02	0.19±0.02	0.27±0.07
MPV	3.87±0.15	3.87±0.23	3.77±0.32	3.57±0.15	3.47±0.12	3.63±0.21
PDW	12.60±0.17	12.03±0.55	11.97±0.91	12.47±0.74	12.50±1.20	12.90±0.56
LYM	0.80±0.53	0.70±0.35	1.17±1.16	0.33±0.12	0.53±0.15	0.43±0.21
MID	0.27±0.06	0.07±0.12	0.20±0.35	0.03±0.06	0.13±0.06	0.10±0.00
GRN	6.80±1.91	5.33±1.61	5.93±0.49	4.50±2.31	4.03±1.65	4.00±0.62
LYM%	9.73±3.43	12.10±9.02	13.70±10.58	8.83±5.95	12.13±7.68	9.90±4.10
MID%	3.33±1.46	1.87±2.45	2.23±3.35	1.07±0.59	3.00±2.10	2.20±0.26
GRN%	86.93±2.32	86.03±11.47	84.07±13.91	99.10±6.34	84.87±9.71	87.90±4.35

Note: Data are presented as mean ± SD (n=3).

Abbreviations: WBC, White blood cells; RBC, Red blood cells; HGB, Hemoglobin; HCT, Hematocrit; MCV, Mean corpuscular volume; MCH, Mean corpuscular hemoglobin; MCHC, Mean corpuscular hemoglobin concentration; RDW, Red cell distribution width; PLT, Platelets; PCT, Plateletcrit; MPV, Mean platelet volume; PDW, Platelet distribution width; LYM, Lymphocytes; MID, Intermediate cell; GRN, Neutrophil granulocyte.

the formation of new blood vessels.^{42,43} Therefore, inhibiting VM channels is a way to inhibit metastasis. In our study, a Matrigel®-based tube formation assay was applied to evaluate the inhibitory effects of treatment with varying liposomal formulations on VM formation. As shown in Figure 5A, dioscin liposomes, daunorubicin and dioscin codelivery liposomes, targeted daunorubicin and dioscin codelivery liposomes caused a substantial degree of damage to the VM channels, and this illustrated that the presence of dioscin could inhibit the formation of VM channels.

Invasion and migration are two significant processes of tumor metastasis. In metastasis, tumor cells detach from the primary site, invade and migrate to the surrounding basement membrane, circulate in the blood or lymphatic system, and finally colonize the distant site.^{44–46} Thus, the inhibition of invasion and migration can significantly prolong the survival of patients. A wound healing assay was performed in vitro to evaluate the inhibitory effects of liposomes on A549 cell invasion. In the blank control group, A549 cells exhibited distinct wound healing abilities. However, formidable inhibitory effects were observed after treatment with dioscin-loaded liposomes, which suggested that the presence of dioscin could dramatically inhibit A549 cell invasion (Figure 5B). In addition, acting as a simulation of the basement membrane, Transwell chambers were established to evaluate the inhibitory effects of liposomes on A549 cell migration. The results showed that all dioscin-loaded formulations suppressed A549 cell migration (Figure 5C), and the number of cells penetrating the Transwell chambers was negligible. These two assays further verified that dioscin played a crucial role in inhibiting tumor metastasis on A549 cells.

The mechanism of tumor metastasis involves the interaction of diverse genes and proteins. MMP-2, which plays a critical role in tumor metastasis, is overexpressed in lung cancer.⁴⁷ MMP-2 degrades the extracellular matrix, destroys the tumor microenvironment and promotes the formation of VM. VE-cad is a transmembrane glycoprotein that can maintain an intercellular connection and is expressed only in highly aggressive tumors. It has been demonstrated that the downregulation of VE-cad can inhibit VM formation.⁴⁸ TGF- β 1 is a cytokine which is secreted by epithelial cells, macrophages and fibroblasts. It can reduce cell adhesion, and thus plays an important role in tumor metastasis.⁴⁹ HIF-1 α can induce VM formation under anoxic conditions, and alter the expression of

metastasis-related proteins, resulting in tumor metastasis. In this study, targeted daunorubicin and dioscin codelivery liposomes could regulate the expression of metastasis-related proteins. As shown in Figure 6, the expression levels of MMP-2, VE-cad, TGF- β 1 and HIF-1 α were obviously downregulated after treatment with the targeted daunorubicin and dioscin codelivery liposomes. These results suggested that the targeted liposomes could inhibit tumor metastasis by regulating the expression of metastasis-related proteins.

Apoptosis, which is also called programmed cell death, is defined as the death of cells under physiological or pathological conditions, and apoptosis induction has been conducted as a strategy to treat tumors.⁵⁰ As an anthracycline chemotherapy drug, the antitumor effect of daunorubicin is realized by inducing apoptosis and inhibiting synthesis of DNA and RNA.⁵¹ To observe apoptosis induced by the varying liposomal formulations, an Annexin V-FITC/PI kit was used to perform double staining. Annexin V is a Ca²⁺ dependent phospholipid binding protein that binds specifically to phosphatidylserine, and it flips out of the membrane during apoptosis. PI is a nucleic acid dye, which can penetrate the damaged cell membrane of late apoptotic cells or necrotic cells. Therefore, Annexin V-FITC/PI can be used to detect early apoptosis and late apoptosis. In the flow cytometry quadrantal diagram, Annexin V⁺/PI⁻ cells are regarded as early apoptotic cells and the Annexin V⁺/PI⁺ cells are regarded as late apoptotic or necrotic cells.³⁷ As shown in Figure 7A, targeted daunorubicin and dioscin codelivery liposomes showed the strongest apoptosis-inducing effects on A549 cells among all liposomal formulations. The highest fluorescence intensity in targeted daunorubicin and dioscin codelivery liposomes group in Figure 7C demonstrated that the apoptosis triggered by the liposomes could be associated with the generation of ROS. The apoptosis assay result confirmed the cytotoxicity induced by varying liposomal formulations.

To observe the distributions of the drug-loaded liposomes in tumor-bearing mice, real-time images were captured by encapsulating fluorescent DiR dye into the liposomal formulations. As shown in Figure 8, we concluded that the liposomal formulations circulated in the blood longer than free DiR did. Targeted DiR liposomes exhibited the strongest tumor targeting ability following the addition of PFV. The antitumor effect in vivo is shown in Figure 9. Targeted daunorubicin and dioscin codelivery

liposomes exhibited the strongest antitumor effect among all the groups (Figure 9B). The body weights of mice in the liposomal groups did not change significantly during treatment, while treatment with free daunorubicin obviously decreased mouse body weights due to the side effects of daunorubicin. The hematological parameters for each group showed no statistically significant differences, which demonstrated the safety of the liposomes. H&E staining, immunohistochemistry and TUNEL assay also proved the enhanced antitumor effects of the targeted daunorubicin and dioscin codelivery liposomes.

Conclusion

In this study, the targeted daunorubicin and dioscin codelivery liposomes were prepared using film dispersion method and ammonium sulfate gradient method. The physicochemical characteristics, inhibition on VM formation, blocking effects on tumor invasion and migration, and antitumor effects were evaluated in vivo and in vitro. As a kind of targeting liposomal drug carrier for NSCLC, it had the following advantages: 1) satisfactory size of approximately 100 nm which was beneficial for tumor targeting due to the EPR effect; 2) enhanced cellular uptake mediated by PFV cell penetrating peptide; 3) increased inhibitory effects on VM formation and tumor metastasis by the addition of dioscin; 4) negligible systemic toxicity at a test dose. Therefore, the targeted daunorubicin and dioscin codelivery liposomes could provide an effective strategy for the treatment of NSCLC.

Acknowledgment

This work was supported by the National Natural Science Foundation of China under Grant No. 81874347.

Disclosure

The authors report no conflicts of interest in this work.

References

- Wong MCS, Lao XQ, Ho K-F, Goggins WB, Tse SLA. Incidence and mortality of lung cancer: global trends and association with socioeconomic status. *Sci Rep*. 2017;7(1):14300. doi:10.1038/s41598-017-14513-7
- Torre LA, Siegel RL, Jemal A. Lung cancer statistics. *Adv Exp Med Biol*. 2016;893:1–19. doi:10.1007/978-3-319-24223-1_1
- Paracha N, Abdulla A, MacGilchrist KS. Systematic review of health state utility values in metastatic non-small cell lung cancer with a focus on previously treated patients. *Health Qual Life Outcomes*. 2018;16(1):179. doi:10.1186/s12955-018-0994-8
- Wang T, Hossann M, Reim HM, et al. In vitro characterization of phosphatidylglycerol-based thermosensitive liposomes with encapsulated 1H MR T1-shortening gadodiamide. *Contrast Media Mol Imaging*. 2008;3(1):19–26. doi:10.1002/cmim.226
- Bunn PA Jr, Soriano A, Johnson G, Heasley L. New therapeutic strategies for lung cancer: biology and molecular biology come of age. *Chest*. 2000;117(Suppl 4):163S–168S. doi:10.1378/chest.117.4_suppl_1.163S
- Sun YW, Xu J, Zhou J, Liu W-J. Targeted drugs for systemic therapy of lung cancer with brain metastases. *Oncotarget*. 2017;9(4):5459–5472. doi:10.18632/oncotarget.23616
- Zhang J, Qiao L, Liang N, et al. Vasculogenic mimicry and tumor metastasis. *J BUON*. 2016;21(3):533–541.
- Owattanapanich W, Owattanapanich N, Kungwankiatichai S, Ungprasert P, Ruchutrakool T. Efficacy and toxicity of idarubicin versus high-dose daunorubicin for induction chemotherapy in adult acute myeloid leukemia: a systematic review and meta-analysis. *Clin Lymphoma Myeloma Leuk*. 2018;18:814–821.e3. doi:10.1016/j.clml.2018.08.008
- Xu PY, Kankala RK, Pan YJ, Yuan H, Wang S-B, Chen A-Z. Overcoming multidrug resistance through inhalable siRNA nanoparticles-decorated porous microparticles based on supercritical fluid technology. *Int J Nanomedicine*. 2018;13:4685–4698. doi:10.2147/IJN.S169399
- Yousefinejad S, Honarasa F, Montaseri H. Linear solvent structure-polymer solubility and solvation energy relationships to study conductive polymer/carbon nanotube composite solutions. *RSC Adv*. 2015;5:42266. doi:10.1039/C4RA14244F
- Kankala RK, Liu CG, Chen AZ. Overcoming multidrug resistance through the synergistic effects of hierarchical pH-sensitive, ROS-generating nanoreactors. *ACS Biomater Sci Eng*. 2017;3(10):2431–2442. doi:10.1021/acsbomaterials.7b00569
- Ying X, Wen H, Lu WL, et al. Dual-targeting daunorubicin liposomes improve the therapeutic efficacy of brain glioma in animals. *J Control Release*. 2010;141(2):183–192. doi:10.1016/j.jconrel.2009.09.020
- Kim JS, Shin DH, Kim JS. Dual-targeting immunoliposomes using angiopep-2 and CD133 antibody for glioblastoma stem cells. *J Control Release*. 2017;269:245–257. doi:10.1016/j.jconrel.2017.11.026
- Li L, Hou J, Liu X, et al. Nucleolin-targeting liposomes guided by aptamer AS1411 for the delivery of siRNA for the treatment of malignant melanomas. *Biomaterials*. 2014;35(12):3840–3850. doi:10.1016/j.biomaterials.2014.01.019
- Xiang B, Jia X-L, Qi J-L, et al. Enhancing siRNA-based cancer therapy using a new pH-responsive activatable cell-penetrating peptide-modified liposomal system. *Int J Nanomedicine*. 2017;12:2385–2405. doi:10.2147/IJN.S129574
- Majumder P, Bhunia S, Chaudhuri A. A lipid-based cell penetrating nano-assembly for RNAi-mediated anti-angiogenic cancer therapy. *Chem Commun*. 2018;54(12):1489–1492. doi:10.1039/C7CC08517F
- Torchilin VP, Levchenko TS, Rammohan R, Volodina N, Papahadjopoulos-Sternberg B, D'Souza GGM. Cell transfection in vitro and in vivo with nontoxic TAT peptide-liposome-DNA complexes. *Proc Natl Acad Sci U S A*. 2003;100(4):1972–1977. doi:10.1073/pnas.0435906100
- Fischer R, Fotin-Mleczek M, Hufnagel H, Brock R. Break on through to the other side-biophysics and cell biology shed light on cell-penetrating peptides. *ChemBiochem*. 2005;6(12):2126–2142. doi:10.1002/cbic.200500044
- Henriques ST, Melo MN, Castanho MA. Cell-penetrating peptides and antimicrobial peptides: how different are they? *Biochem J*. 2006;399(1):1–7. doi:10.1042/BJ20061100
- Yuan M, Qiu Y, Zhang L, Gao H, He Q. Targeted delivery of transferrin and TAT co-modified liposomes encapsulating both paclitaxel and doxorubicin for melanoma. *Drug Deliv*. 2016;23(4):1171–1183. doi:10.3109/10717544.2015.1040527
- Boussoufi F, Navarro Gallón S, Chang R, Webster TJ. Synthesis and study of cell-penetrating peptide-modified gold nanoparticles. *Int J Nanomedicine*. 2018;13:6199–6205. doi:10.2147/IJN.S168720

22. Lin W, Xie X, Yang Y, et al. Thermosensitive magnetic liposomes with doxorubicin cell-penetrating peptides conjugate for enhanced and targeted cancer therapy. *Drug Deliv.* 2016;23(9):3436–3443. doi:10.1080/10717544.2016.1189983
23. Cai D, Gao W, He B, et al. Hydrophobic penetrating peptide PFVYLI-modified stealth liposomes for doxorubicin delivery in breast cancer therapy. *Biomaterials.* 2014;35(7):2283–2294. doi:10.1016/j.biomaterials.2013.11.088
24. Lakkadwala S, Singh J. Co-delivery of doxorubicin and erlotinib through liposomal nanoparticles for glioblastoma tumor regression using an in vitro brain tumor model. *Colloids Surf B Biointerfaces.* 2018;173:27–35. doi:10.1016/j.colsurfb.2018.09.047
25. Watkins CL, Brennan P, Fegan C, et al. Cellular uptake, distribution and cytotoxicity of the hydrophobic cell penetrating peptide sequence PFVYLI linked to the proapoptotic domain peptide PAD. *J Control Release.* 2009;140(3):237–244. doi:10.1016/j.jconrel.2009.04.028
26. Lin S, Wang D, Yang D, Yao J, Tong Y, Chen J. Characterization of steroidal saponins in crude extract from *Dioscorea nipponica* Makino by liquid chromatography tandem multi-stage mass spectrometry. *Anal Chim Acta.* 2007;599(1):98–106. doi:10.1016/j.aca.2007.07.070
27. Sun W, Tu G, Zhang Y. A new steroidal saponin from *Dioscorea zingiberensis* Wright. *Nat Prod Res.* 2003;17(4):287–292. doi:10.1080/1478641031000136997
28. Tao X, Yin L, Xu L, Peng J. Dioscin: a diverse acting natural compound with therapeutic potential in metabolic diseases, cancer, inflammation and infections. *Pharmacol Res.* 2018;137:259–269. doi:10.1016/j.phrs.2018.09.022
29. Lim WC, Kim H, Kim YJ, et al. Dioscin suppresses TGF- β 1-induced epithelial-mesenchymal transition and suppresses A549 lung cancer migration and invasion. *Bioorg Med Chem Lett.* 2017;27(15):3342–3348. doi:10.1016/j.bmcl.2017.06.014
30. Aumsuwan P, Khan SI, Khan IA, et al. The anticancer potential of steroidal saponin, dioscin, isolated from wild yam (*Dioscorea villosa*) root extract in invasive human breast cancer cell line MDA-MB-231 in vitro. *Arch Biochem Biophys.* 2016;591:98–110. doi:10.1016/j.abb.2015.12.001
31. Kou Y, Ji L, Wang H, et al. Connexin 43 upregulation by dioscin inhibits melanoma progression via suppressing malignancy and inducing M1 polarization. *Int J Cancer.* 2017;141(8):1690–1703. doi:10.1002/ijc.30872
32. Si L, Zheng L, Xu L, et al. Dioscin suppresses human laryngeal cancer cells growth via induction of cell-cycle arrest and MAPK-mediated mitochondrial-derived apoptosis and inhibition of tumor invasion. *Eur J Pharmacol.* 2016;774:105–117. doi:10.1016/j.ejphar.2016.02.009
33. Liu S, Zhang SM, Ju RJ, et al. Antitumor efficacy of Lf modified daunorubicin plus honokiol liposomes in treatment of brain glioma. *Eur J Pharm Sci.* 2017;106:185–197. doi:10.1016/j.ejps.2017.06.002
34. Song XL, Ju RJ, Xiao Y, et al. Application of multifunctional targeting epirubicin liposomes in the treatment of non-small-cell lung cancer. *Int J Nanomedicine.* 2017;12:7433–7451. doi:10.2147/IJN.S141787
35. Ju RJ, Cheng L, Peng XM, et al. Octreotide-modified liposomes containing daunorubicin and dihydroartemisinin for treatment of invasive breast cancer. *Artif Cells Nanomed Biotechnol.* 2018;46:616–628. doi:10.1080/21691401.2018.1433187.
36. Yang J, Li W, Luo L, et al. Hypoxic tumor therapy by hemoglobin-mediated drug delivery and reversal of hypoxia-induced chemoresistance. *Biomaterials.* 2018;182:145–156. doi:10.1016/j.biomaterials.2018.08.004
37. Li C, Hu J, Li W, Song G, Shen J. Combined bortezomib-based chemotherapy and p53 gene therapy using hollow mesoporous silica nanospheres for p53 mutant non-small cell lung cancer treatment. *Biomater Sci.* 2016;5(1):77–88. doi:10.1039/c6bm00449k
38. Pumerantz AS. PEGylated liposomal vancomycin: a glimmer of hope for improving treatment outcomes in MRSA pneumonia. *Recent Pat Antiinfect Drug Discov.* 2012;7(3):205–212.
39. Luo Q, Yang B, Tao W, et al. ATB⁰⁺ transporter-mediated targeting delivery to human lung cancer cells via aspartate-modified docetaxel-loading stealth liposomes. *Biomater Sci.* 2017;5(2):295–304. doi:10.1039/c6bm00788k
40. Anabousi S, Laue M, Lehr C-M, Bakowsky U, Ehrhardt C. Assessing transferrin modification of liposomes by atomic force microscopy and transmission electron microscopy. *Eur J Pharm Biopharm.* 2005;60(2):295–303. doi:10.1016/j.ejpb.2004.12.009
41. Thakur C, Rapp UR, Rudel T. Cysts mark the early stage of metastatic tumor development in non-small cell lung cancer. *Oncotarget.* 2017;9(5):6518–6535. doi:10.18632/oncotarget.23785
42. Maniotis AJ, Folberg R, Hess A, et al. Vascular channel formation by human melanoma cells in vivo and in vitro: vasculogenic mimicry. *Am J Pathol.* 1999;155(3):739–752. doi:10.1016/S0002-9440(10)65173-5
43. Seftor RE, Hess AR, Seftor EA, et al. Tumor cell vasculogenic mimicry: from controversy to therapeutic promise. *Am J Pathol.* 2012;181(4):1115–1125. doi:10.1016/j.ajpath.2012.07.013
44. Quail DF, Joyce JA. Microenvironmental regulation of tumor progression and metastasis. *Nat Med.* 2013;19(11):1423–1437. doi:10.1038/nm.3394
45. Wan L, Pantel K, Kang Y. Tumor metastasis: moving new biological insights into the clinic. *Nat Med.* 2013;19(11):1450–1464. doi:10.1038/nm.3391
46. Schroeder A, Heller DA, Winslow MM, et al. Treating metastatic cancer with nanotechnology. *Nat Rev Cancer.* 2011;12(1):39–50. doi:10.1038/nrc3180
47. Deryugina EI, Quigley JP. Matrix metalloproteinases and tumor metastasis. *Cancer Metastasis Rev.* 2006;25(1):9–34. doi:10.1007/s10555-006-7886-9
48. Cappelli HC, Kanugula AK, Adapala RK, et al. Mechanosensitive TRPV4 channels stabilize VE-cadherin junctions to regulate tumor vascular integrity and metastasis. *Cancer Lett.* 2018;442:15–20. doi:10.1016/j.canlet.2018.07.042
49. Ko H, So Y, Jeon H, et al. TGF- β 1-induced epithelial-mesenchymal transition and acetylation of Smad2 and Smad3 are negatively regulated by EGCG in human A549 lung cancer cells. *Cancer Lett.* 2013;335(1):205–213. doi:10.1016/j.canlet.2013.02.018
50. Li R, Shi Y, Zhao S, et al. NF- κ B signaling and integrin- β 1 inhibition attenuates osteosarcoma metastasis via increased cell apoptosis. *Int J Biol Macromol.* 2018;123:1035–1043. doi:10.1016/j.ijbiomac.2018.11.003.
51. Lotfi K, Zackrisson AL, Peterson C. Comparison of idarubicin and daunorubicin regarding intracellular uptake, induction of apoptosis, and resistance. *Cancer Lett.* 2002;178(2):141–149.

International Journal of Nanomedicine

Dovepress

Publish your work in this journal

The International Journal of Nanomedicine is an international, peer-reviewed journal focusing on the application of nanotechnology in diagnostics, therapeutics, and drug delivery systems throughout the biomedical field. This journal is indexed on PubMed Central, MedLine, CAS, SciSearch[®], Current Contents[®]/Clinical Medicine,

Journal Citation Reports/Science Edition, EMBase, Scopus and the Elsevier Bibliographic databases. The manuscript management system is completely online and includes a very quick and fair peer-review system, which is all easy to use. Visit <http://www.dovepress.com/testimonials.php> to read real quotes from published authors.

Submit your manuscript here: <https://www.dovepress.com/international-journal-of-nanomedicine-journal>